IL-15 superagonist/IL-15RαSushi-Fc fusion complex (IL-15SA/IL-15RαSu-Fc; ALT-803) markedly enhances specific sub-populations of NK and memory CD8+ T cells, and mediates potent anti-tumor activity against murine breast and colon carcinomas

Peter S. Kim[1], Anna R. Kwilas[1], Wenxin Xu[2], Sarah Alter[2], Emily K. Jeng[2], Hing C. Wong[2], Jeffrey Schlom[1,*], James W. Hodge[1,*]

[1]Laboratory of Tumor Immunology and Biology, Center for Cancer Research, National Cancer Institute, National Institutes of Health, Bethesda, MD, USA

[2]Altor BioScience Corporation, Miramar, FL, USA

[*]These authors have contributed equally to this work

Correspondence to: James W. Hodge, *e-mail:* jh241d@nih.gov

ABSTRACT

Interleukin (IL)-15-N72D superagonist-complexed with IL-15RαSushi-Fc fusion protein (IL-15SA/IL-15RαSu-Fc; ALT-803) has been reported to exhibit significant anti-tumor activity in murine myeloma, rat bladder cancer, and murine glioblastoma models. In this study, we examined the immunomodulatory and anti-tumor effects of IL-15SA/IL-15RαSu-Fc in tumor-free and highly metastatic tumor-bearing mice. Here, IL-15SA/IL-15RαSu-Fc significantly expanded natural killer (NK) and CD8+ T cells. In examining NK cell subsets, the greatest significant increase was in highly cytotoxic and migrating (CD11b+, CD27hi; high effector) NK cells, leading to enhanced function on a per-cell basis. CD8+ T cell subset analysis determined that IL-15SA/IL-15RαSu-Fc significantly increased IL-15 responding memory (CD122+, CD44+) CD8+ T cells, in particular those having the innate (NKG2D+, PD1−) phenotype. In 4T1 breast tumor–bearing mice, IL-15SA/IL-15RαSu-Fc induced significant anti-tumor activity against spontaneous pulmonary metastases, depending on CD8+ T and NK cells, and resulting in prolonged survival. Similar anti-tumor activity was seen in the experimental pulmonary metastasis model of CT26 colon carcinoma cells, particularly when IL-15SA/IL-15RαSu-Fc was combined with a cocktail of checkpoint inhibitors, anti-CTLA-4 and anti-PD-L1. Altogether, these studies showed for the first time that IL-15SA/IL-15RαSu-Fc (1) promoted the development of high effector NK cells and CD8+ T cell responders of the innate phenotype, (2) enhanced function of NK cells, and (3) played a vital role in reducing tumor metastasis and ultimately survival, especially in combination with checkpoint inhibitors.

INTRODUCTION

IL-15 is a pleiotropic cytokine that has been shown to induce and regulate a wide range of immune functions [1, 2]. Specifically, IL-15 is critical for lymphoid development and peripheral maintenance of innate immune cells and immunological memory of T cells, in particular natural killer (NK) and CD8+ T cell populations [1, 2]. However, while IL-15 does not promote the maintenance

of CD4+ CD25+ FOXP3+ regulatory T cells (Tregs), IL-2 has been demonstrated to induce their development [3–5]. Furthermore, IL-15 has been shown to protect effector T cells from IL-2–mediated activation-induced cell death (AICD) [6, 7]. For these reasons, IL-15 has long been speculated to have high therapeutic potential for long-term anti-tumor immunity. The cytokine's immune effect in cancer patients has been recently examined. In a first-in-human clinical trial of recombinant human (rh)IL-15,

Conlon et al. found that rhIL-15 administration induced a 10-fold expansion of NK cells and significantly increased the proliferation of γδT cells and CD8+ T cells [8].

Despite its promising anti-tumor immune capacity, IL-15 has been shown to exhibit a short half-life and high doses were required to achieve biological responses *in vivo* [9, 10], hence resulting in clinical toxicities and limited anti-tumor responses in patients [8]. To increase the therapeutic effectiveness and facilitate the use of IL-15 in the immunotherapy of cancer and chronic infection, an IL-15 N72D superagonist/IL-15RαSushi-Fc fusion complex (IL-15SA/IL-15RαSu-Fc; ALT-803) has been developed to address some of the limitations of IL-15–based therapeutics. First, in the IL-15 N72D superagonist (IL-15SA), the asparagine 72 was replaced with the aspartic acid residue, providing improved affinity for CD122-expressing immune cells and promoting stronger cytoplasmic signals for activation and proliferation of NK and CD8+ T cells at lower dosages [11]. Furthermore, it has been previously shown that the biological activity of IL-15 increased when IL-15 was pre-complexed with IL-15Rα [12, 13]. Simulating trans-presentation between dendritic cells/macrophages and effector cells, the sushi domain of IL-15Rα, fused to the Fc portion of human IgG1 [11], has been engineered to incorporate the trans-presentation mechanism, consequently increasing the half-life and *in vivo* biological activity of the IL-15-SA [11, 14]. Overall, when compared with native IL-15, the IL-15SA/IL-15RαSu-Fc fusion complex has been shown to exhibit a longer serum half-life and retention in lymphoid organs and increased *in vivo* biological activity by 5–25-fold [11, 14, 15].

Due to its potent immunostimulatory capability, the IL-15SA/IL-15RαSu-Fc fusion complex has been shown to be efficacious in several experimental animal models of cancer, namely murine multiple myeloma [16], rat bladder cancer [17], and murine glioblastoma [18], and currently is being tested against human hematological and solid cancers in multiple clinical trials (ClinicalTrials.gov). Here, we evaluated for the first time, (1) the immunomodulatory effect of IL-15SA/IL-15RαSu-Fc on the subpopulations of NK cells (and memory CD8+ T cells) and (2) its anti-tumor activity against pulmonary metastases in the 4T1 breast and CT26 colon carcinoma models, with the aim of providing a rationale for the utilization of IL-15SA/IL-15RαSu-Fc, especially in combination with checkpoint inhibitors, in the immunotherapy of highly metastatic cancers.

RESULTS

IL-15SA/IL-15RαSu-Fc induced marked elevations of TH_1 and TH_2 cytokines

Due to the pleiotropic nature of IL-15 in regulating various immune responses, we first sought to examine the extent to which IL-15SA/IL15-RαSu-Fc promoted the production of Th1 and Th2 cytokines over a 7-day period. Mice administered with IL-15SA/IL15RαSu-Fc exhibited a transient increase in the serum concentration levels of IFN-γ, TNF-α, IL-5, and IL-10 (Figure 1A). Serum IFN-γ level, in particular, peaked on day 1 ($p = 0.004$), followed by IL-5 and IL-10 on day 2 ($p = 0.005$ and $p = 0.030$, respectively), then TNF-α on day 3 ($p = 0.001$) (Figure 1A). There was no significant change observed in serum IL-6 level (Figure 1A; inset). The greatest fold change was observed for IFN-γ, whose fold increase was as high as ~11-fold ($p = 0.004$) on day 1, whereas the other cytokines did not increase beyond 5-fold during the 7-day period (Figure 1B). The duration of elevated serum cytokine level was the greatest for TNF-α, maintaining significantly above the baseline on day 7 ($p = 0.001$), and the shortest for IFN-γ, lasting up to day 4 ($p = 0.028$) (Figure 1A). Even though administration of IL-15SA/IL-15RαSu-Fc to mice rapidly increased inflammatory cytokines at the dose described, no observable toxicities were seen in mice throughout the 7-day period.

IL-15SA/IL-15RαSu-Fc promoted the expansion of NK, T, B cell and granulocytic populations in the spleen

Next, we examined the effect of IL-15SA/IL15RαSu-Fc on major immune populations in the spleen. Administration of IL-15SA/IL-15RαSu-Fc to mice induced the greatest effect on NK cells, whose increase in the total number was highest on day 3 ($p = 0.003$) and lasted markedly above the baseline up to day 5 ($p < 0.001$). T and B cells were similarly affected, as the total numbers of CD8+ and conventional (conv.) CD4+ T cells increased, peaking on day 3 (CD8+: $p = 0.007$; conv.CD4+: $p = 0.013$), whereas B cells and regulatory CD4+ T cells (Tregs) peaked on day 2 (B cells: $p = 0.003$; Tregs: $p = 0.018$) then plateaued until day 4 (B cells: $p = 0.020$; Tregs: $p = 0.006$) (Figure 2A). Among these lymphocytes, the highest fold change was observed in NK cells (~13 fold on day 3; $p = 0.003$) followed by CD8+ T cells (~3 fold on day 3; $p = 0.007$) then CD4+ (conv. and Tregs) T and B cells. We also examined the effect of IL-15SA/IL-15RαSu-Fc on granulocytic and monocytic populations. The total number of CD11b+ Ly-6C^{int} Ly-6G+ cells, identified as either neutrophils or granulocytic myeloid derived suppressor cells (MDSCs), increased as high as 6-fold on day 2 ($p = 0.002$), whereas CD11b+ Ly-6C^{hi} Ly-6G− cells, characterized either as monocytes or monocytic-MDSCs, appeared to be unaffected by IL-15SA/IL-15RαSu-Fc. IL-15SA/IL-15RαSu-Fc similarly enhanced the expansion of NK cells in PBMCs in comparison with those in the spleens (Supplemental Figure 1). Taken together these data are consistent with the overall immunomodulatory property of IL-15, which activates both the innate and adaptive arms of the immune system [2, 19].

IL-15SA/IL-15RαSu-Fc most affected IL-15-responding memory T cells, specifically of the innate phenotype in the CD8+ T cell compartment

We observed that even though the total numbers of both CD8+ and CD4+ T cells increased, partly as a result of overall increase in the total number of splenocytes, the fold increase was greater in CD8+ than in CD4+ T cells or splenocytes (Figure 2B). We therefore investigated which splenic T cell subsets, in particular in the CD8+ compartment, responded to IL-15SA/IL-15RαSu-Fc treatment. More specifically, we sought to

examine the following phenotypically defined T cell subsets: (1) IL-15–responding memory T cells identified by the IL-15 receptor β-chain, CD122, and the antigen-experienced memory marker, CD44, (2) innate IL-15-responding memory T cells characterized by expression of the NK-activating receptor, NKG2D, on CD122+ CD44+ T cells, and (3) adaptive IL-15-responding memory T cells identified by an immunoinhibitory receptor, PD-1, which upregulates upon T cell receptor (TCR) ligation on CD122+ CD44+ T cells. Within the CD8+ T cell population, IL-15SA/IL-15RαSu-Fc significantly increased IL-15 memory responders (CD122+ CD44+; up to ~15 fold on day 3; $p = 0.014$;
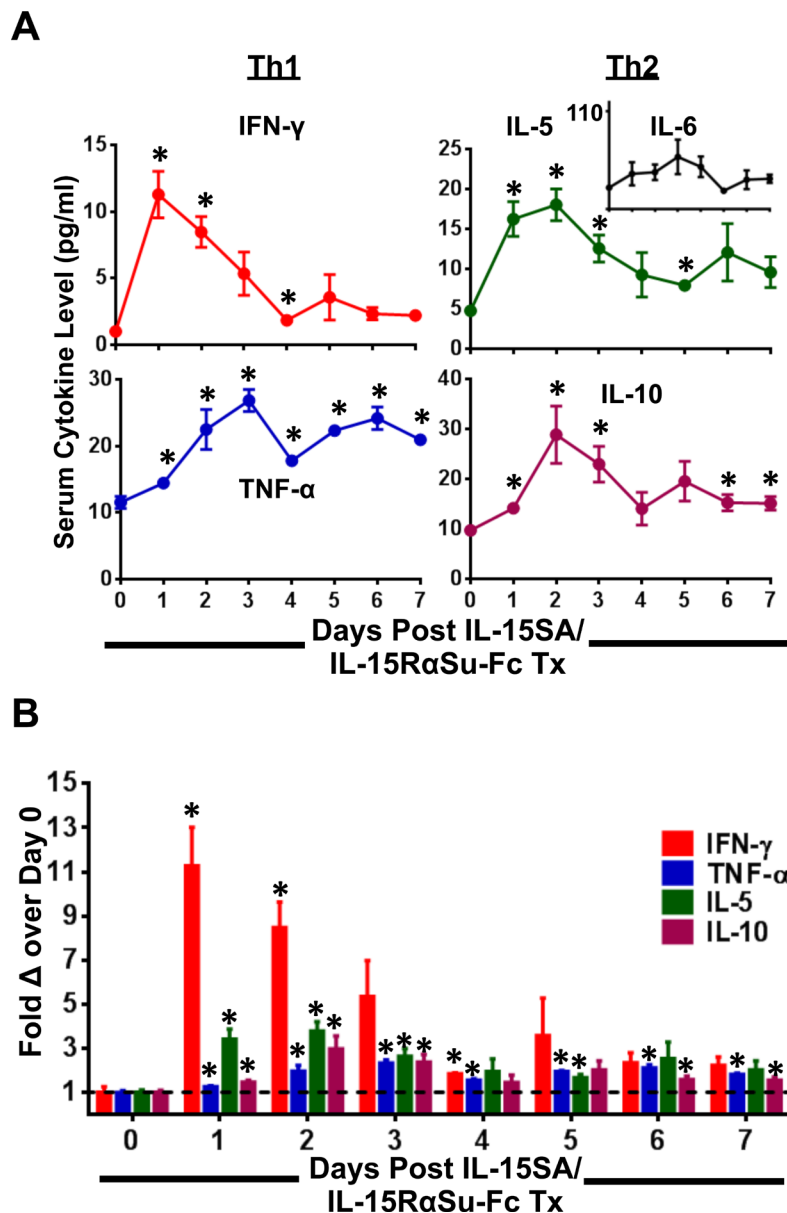

Figure 1: IL-15SA/IL-15RαSu-Fc markedly induces TH$_1$ and TH$_2$ cytokines. A multiplex cytokine analysis is shown, measuring **A.** serum cytokine concentrations of IFN-γ, TNF-α, IL-5 and IL-10 as well as **B.** their fold changes over a 7-day period post treatment in female Balb/c mice (n=3/group). Serum IL-6 level is shown as an inset in (A). *$p < 0.05$, statistical significance.

Figure 3B) whose immune response profile was very similar to that of NK cells (Figures 2 and 3). Within IL-15 memory CD8$^+$ T cell responders, those of the innate phenotype (NKG2D$^+$ PD1$^-$) increased dramatically as high as ~70 fold on day 3 (p = 0.012) (Figure 3B), also having response kinetics similar to that seen in NK cells. However, IL-15SA/IL-15RαSu-Fc did not have a similar magnitude of effect on these subsets in the CD4$^+$ T cell compartment (Figure 3A). Finally, in both CD8$^+$ and CD4$^+$ T cell compartments, IL-15SA/IL-15RαSu-Fc had
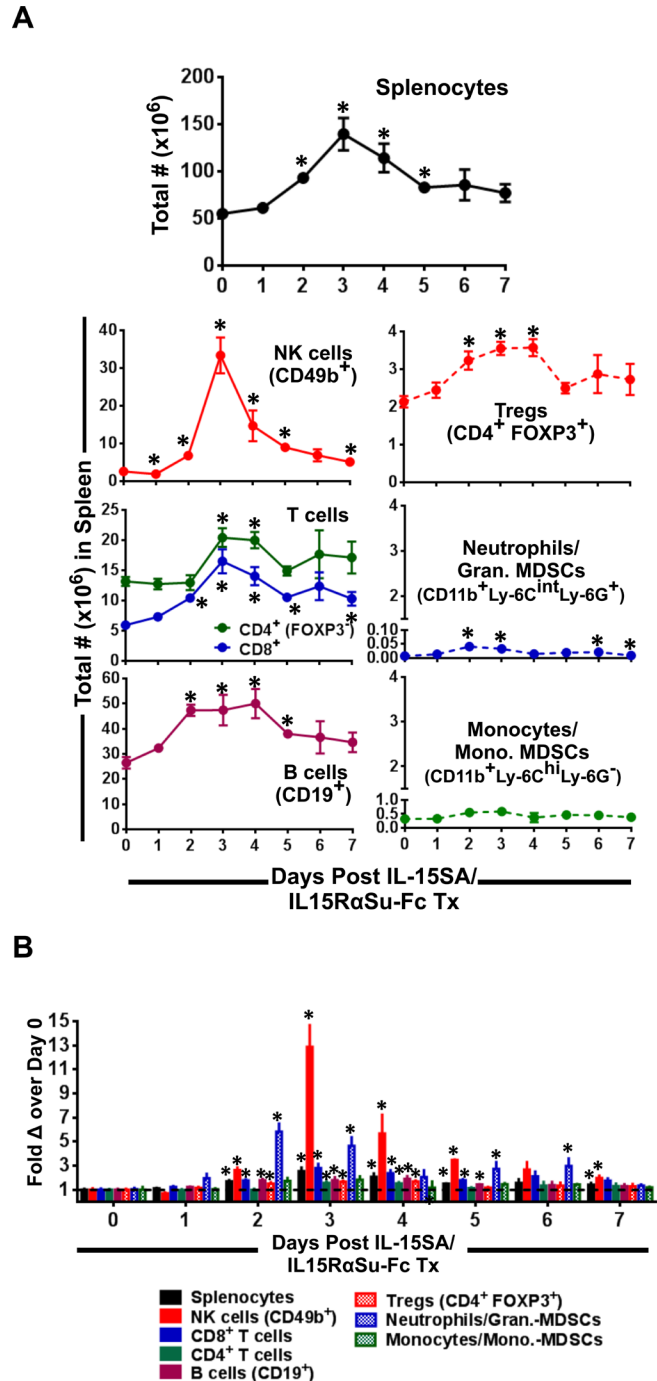

Figure 2: IL-15SA/IL-15RαSu-Fc significantly induces the expansion of splenic NK, T, B cell and granulocytic populations. A. The total numbers of splenocytes, NK (CD49b$^+$) cells, T (CD8$^+$ and CD4$^+$) cells, B (CD19$^+$) cells, Tregs (CD4$^+$ FOXP3$^+$), neutrophils/granulocytic MDSCs (CD11b$^+$ Ly-6C^{int} Ly-6G$^+$) and monocytes/monocytic MDSCs (CD11b$^+$ Ly-6C^{hi}, Ly-6G$^-$) as well as **B.** their fold changes are shown over a 7-day period post treatment in female Balb/c mice (n=3/group). *p < 0.05, statistical significance. This experiment was repeated at least 2 times with similar results.

an effect on IL-15 memory responders with the adaptive phenotype (NKG2D⁻ PD1⁺), but not to the same degree of magnitude as those with the innate phenotype (Figure 3B). These data are in line with IL-15SA/IL-15RαSu-Fc's capacity to convert antigen-experienced memory CD8⁺ T cells into non-antigen-specific innate effector cells as demonstrated by Xu et al. [16].

IL-15-SA/IL-15RαSu-Fc promoted the development of "high effector" (CD11b⁺ CD27ʰⁱ) NK cells

Because IL-15SA/IL-15RαSu-Fc induced a potent expansion of NK cells in the spleen (Figure 2), we next investigated which splenic NK subset(s) most
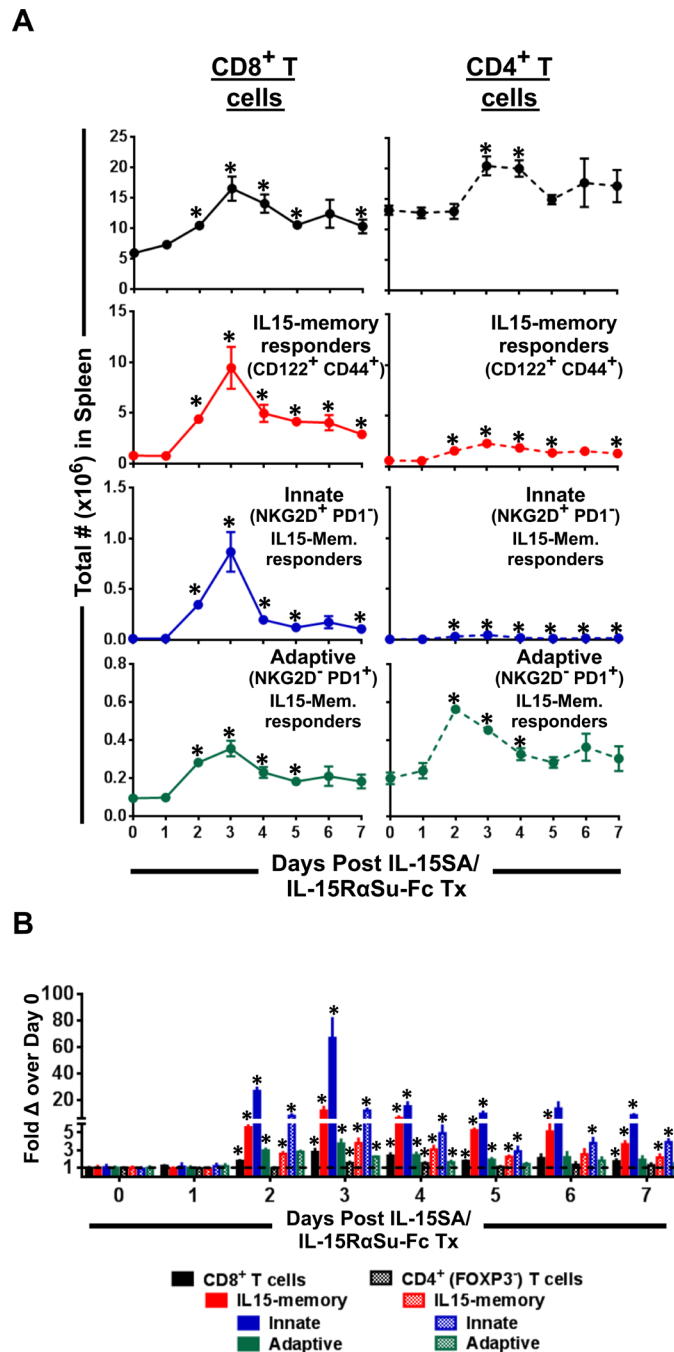

Figure 3: IL-15SA/IL-15RαSu-Fc increases IL-15 memory responders in splenic CD8⁺ T cell population, in particular those with the innate phenotype. A. The total numbers of IL-15 memory responders (CD122⁺ CD44⁺) plus their innate (NKG2D⁺ PD1⁻) and adaptive (NKG2D⁻ PD1⁺) subsets in splenic CD8⁺ and CD4⁺ T cell populations as well as **B.** their fold changes are shown over a 7-day period post treatment in female Balb/c mice (n=3/group). *$p < 0.05$, statistical significance. This experiment was repeated at least 2 times with similar results.

responded to IL-15SA/IL-15RαSu-Fc treatment. We found that unlike CD8^{+} T cells, nearly all NK cells throughout the 7-day period of IL-15SA/IL-15RαSu-Fc–mediated immune response had an activated phenotype (CD122^{+} NKp46^{+}), leading us to further phenotype the NK population using CD11b and CD27 surface markers [20]. It has been reported that CD11b^{+} CD27^{hi} NK cells were resistant to self–major histocompatibility complex (MHC) class I–induced tolerance and exhibited high cytotoxicity, cytokine production and migratory capacity [20–23], hence termed "high effector" NK cells. On the other hand, CD11b^{+} CD27^{lo} or "terminal effector" NKs, albeit having high cytolytic activity, produced low levels of cytokines, were less migratory, and highly expressed the terminal differentiation marker KLRG-1 [20–23]. The results showed that IL-15SA/IL-15RαSu-Fc significantly increased the total numbers of both high (CD11b^{+} CD27^{hi}) and terminal (CD11b^{+} CD27^{lo}) effector NK cells, peaking on day 3 (high effectors: $p = 0.001$;

terminal effectors: $p = 0.008$) (Figure 4A), and the highest fold increase was observed in high effector NK cells (up to ~20 fold on day 3; $p = 0.001$; Figure 4B). The capacity of IL-15SA/IL-15RαSu-Fc to generate high effector NK cells suggests that per-cell NK function may be increased as a result of the cytokine complex treatment.

IL-15SA/IL-15RαSu-Fc increased total NK cells and function on a per-cell basis

Because IL-15SA/IL-15RαSu-Fc expanded high effector NK cells, we next investigated the effect of IL-15SA/IL-15RαSu-Fc on total and per-cell function of NK cells. On day 3, the proportion of high effector NK cells increased (~2-fold on day 3), resulting in decreased proportions of other NK subsets (Figure 5A). When we examined the total NK activity using day 3 splenocytes as effectors and YAC-1 cells as targets, IL-15SA/IL-
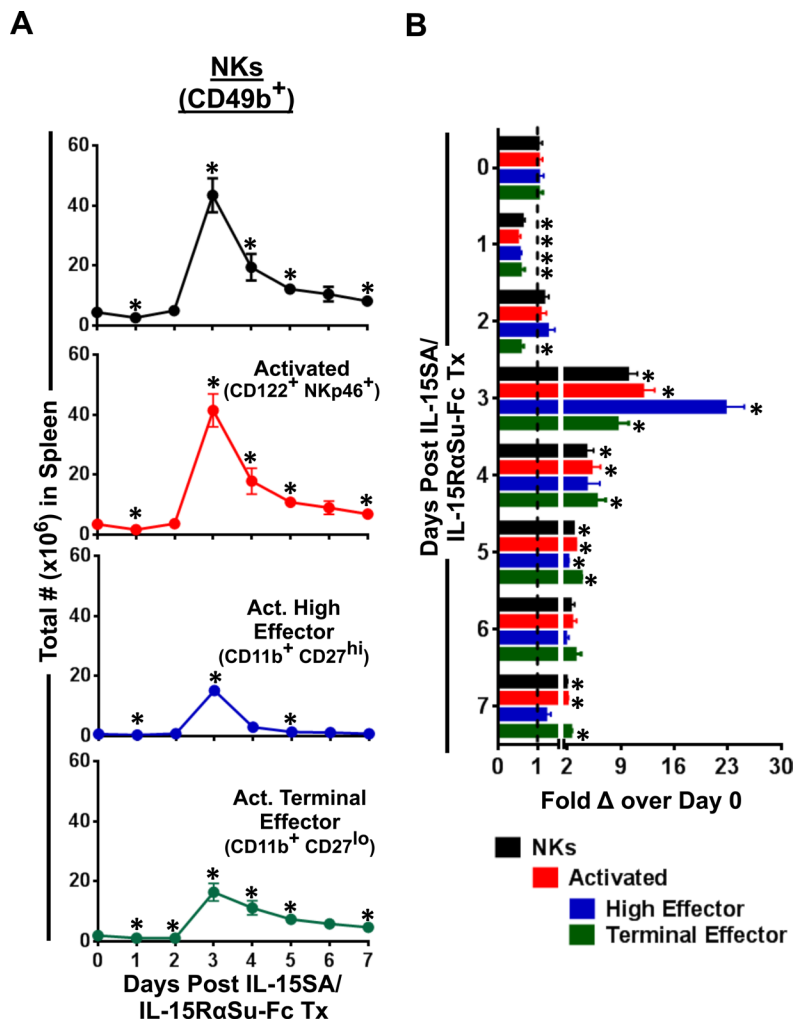

Figure 4: IL-15SA/IL-15RαSu-Fc enhances the development of "high effector" NK cells. A. The total numbers of NK (CD49b^{+}) cells, activated (CD122^{+} NKp46^{+}) NK cells, activated "high effector" (CD11b^{+} CD27^{hi}) and "terminal effector" (CD11b^{+} CD27^{lo}) NK cells over a 7-day period post treatment in female Balb/c mice (n=3/group) as well as **B.** their fold changes are shown. *$p < 0.05$, statistical significance. This experiment was repeated at least 2 times with similar results.

15RαSu-Fc dramatically increased total NK-mediated cytotoxicity (E:T/100:1, $p = 0.004$) (Figure 5B), which was consistent with the increased percentage of splenic NK cells from the IL-15SA/IL-15RαSu-Fc treatment group (~4-fold on day 3; Figure 4A). We then purified NK cells from the spleens (purity: ~85%) on day 3 to determine the effect of IL-15SA/IL-15RαSu-Fc on NK cells on a per-cell basis (Figure 5C). The results indicated that IL-15SA/IL-15RαSu-Fc significantly enhanced the per-cell function of NK cells (E:T/100:1, $p< 0.001$), mediated in large part by the presence of NKG2D, as the per-cell NK-mediated lytic activity (IL-15SA/IL-15RαSu-Fc: 50 LU vs. Isotype Ctrl: 5 LU) decreased when a blocking NKG2D antibody was used (Figure 5D). These studies indicate that IL-15SA/IL-15RαSu-Fc has the potential to induce a potent NK-mediated anti-tumor response due to its ability to enhance not only total NK function but also per-cell NK function through the generation of high effector NKs.

We next conducted studies in tumor-bearing mice to determine if treatment with IL-15SA/IL-15RαSu-Fc would impact immune cell populations to a similar degree as observed in non-tumor-bearing mice. We utilized the spontaneous metastasis model of 4T1 breast carcinoma. We injected 1 µg of IL-15SA/IL-15RαSu-Fc on day 7 post–tumor implantation when the primary tumor size ranged between 50-100 mm³ and harvested splenocytes 3 days later (3 day post ALT-803 administration/day10 post tumor implantation. Primary tumor volumes on day 10 post tumor challenge were ~100 mm³ for both
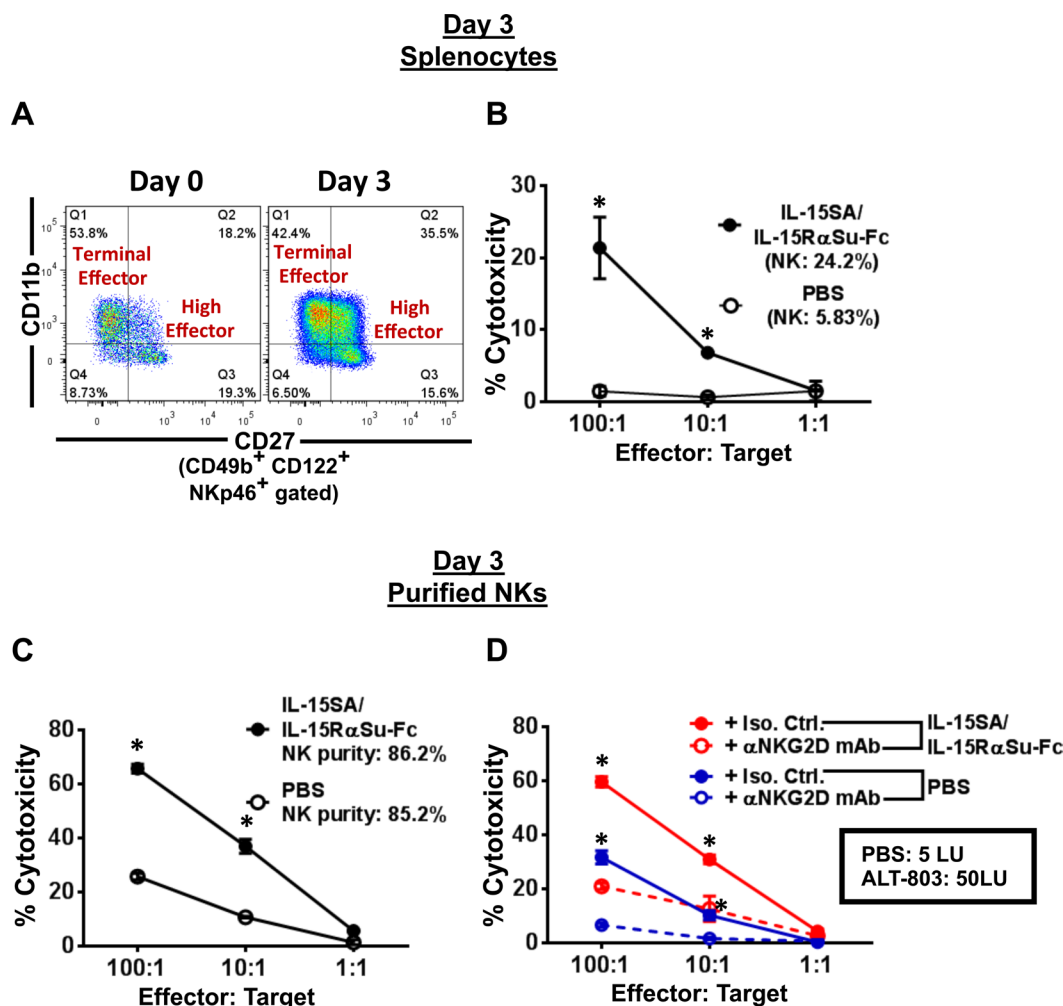

Figure 5: IL-15SA/IL-15RαSu-Fc increases the total-cell as well as per-cell function of NK cells, dependent on NKG2D. Female Balb/c mice ($n = 5–10$/group) were given a single injection of PBS or IL-15-SA/IL-15RαSu-Fc, and the spleens were harvested on day 3 post-treatment. **A.** A representative flow analysis of splenic NK cell subsets from PBS and IL-15-SA/IL-15RαSu-Fc–treated mice is shown. **B.** Bulk splenocytes were used as effectors and co-cultured with YAC-1 target cells at 100:1, 10:1, and 1:1 effector-to-target ratios. [111]In radioactivity was measured to determine cytotoxic function. **C.** Purified splenic NK cells were used as effectors in the cytotoxicity assay described in (B). **D.** Anti-mouse NKG2D mAb or its isotype control were added in the cytotoxicity assay described in (C); NK activity in lytic units (LU). All experiments were performed twice with similar results. Error bars represent SE of mean of quadruplicate measurements. *$p < 0.05$, statistical significance. This experiment was repeated 2 times with similar results.

ALT-803 and PBS treatment groups. As in non-tumor bearing mice, administration of IL-15SA/IL-15RαSu-Fc to mice induced the greatest effect on NK cells (3.5 fold, $p < 0.001$), followed by a significant increase in CD8^{+} and CD4^{+} T-cells (Figure 6A and 6B). Tregs were not significantly increased. When total NK activity was analyzed using day 3 splenocytes as effectors and 4T1 tumor cells as targets, IL-15SA/IL-15RαSu-Fc dramatically increased total NK-mediated cytotoxicity (Figure 6C), (E:T/100:1, $p <0.001$). Similar results were observed using enriched NK cells from the spleens of IL-15SA/IL-15RαSu-Fc treated tumor-bearing mice. These studies indicate that IL-15SA/IL-15RαSu-Fc has the potential to induce a potent NK-mediated anti-tumor response due to its ability to enhance total NK function in tumor-bearing mice.

IL-15SA/IL-15RαSu-Fc showed significant anti-metastatic activity, dependent on CD8^{+} T cells as well as NK cells, and prolonged survival in 4T1 breast tumor model

To assess the functional consequences of IL-15SA/IL-15RαSu-Fc–mediated anti-tumor immunity and efficacy, we used the spontaneous metastasis model of 4T1 breast carcinoma, as the progressive invasion of 4T1 tumor cells to draining lymph nodes and other organs is similar to that seen in the advanced breast cancer in humans [24, 25]. We injected 1 µg of IL-15SA/IL-15RαSu-Fc on day 7 post–tumor implantation when the primary tumor size ranged between 50-100 mm³. IL-15SA/IL-15RαSu-Fc did not affect the primary tumor growth, but generated significant anti-metastatic activity, as the number of 4T1
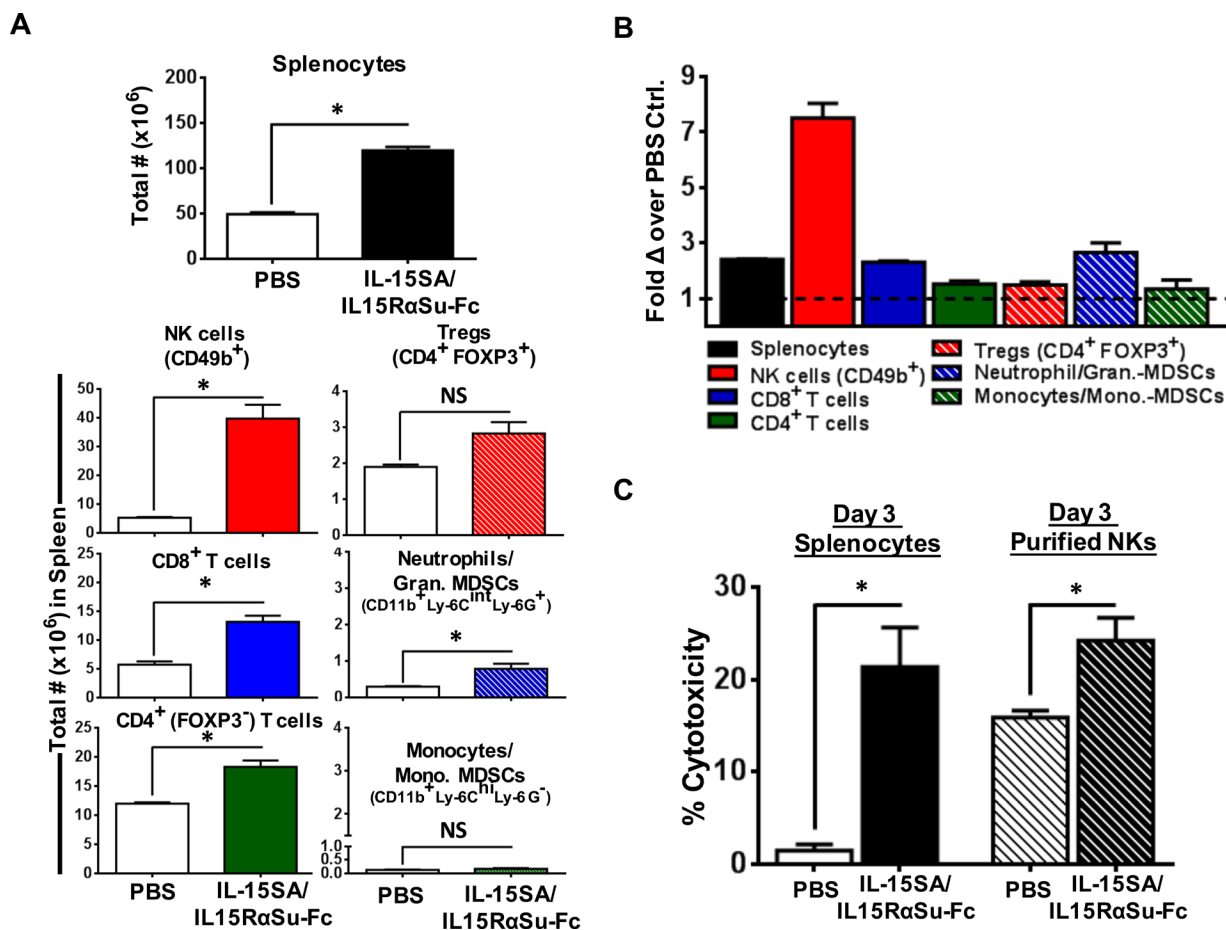

Figure 6: IL-15SA/IL-15RαSu-Fc significantly promotes the expansion of splenic lymphocyte and granulocyte populations in 4T1 tumor-bearing mice and increases *ex vivo* NK cytotoxicity against 4T1 tumor cells on total and per cell basis. A. Female Balb/c mice (n=3/group) received 4T1 mammary tumor cells, then IL-15SA/IL-15RαSu-Fc or PBS on day 7 post–tumor implantation. On day 10, the spleens were harvested for immune analysis. The total numbers of splenocytes, NK (CD49b^{+}) cells, T (CD8^{+} and CD4^{+}) cells, Tregs (CD4^{+} FOXP3^{+}), neutrophils/granulocytic MDSCs (CD11b^{+} Ly-6C^{int} Ly-6G^{−}) and monocytes/monocytic MDSCs (CD11b^{+} Ly-6C^{hi}, Ly-6G^{+}) as well as **B.** their fold changes are shown. **C.** Female Balb/c mice (n = 5–10/group) were given a single injection of IL-15-SA/IL-15RαSu-Fc or PBS, and the spleens were harvested on day 3 post-treatment. Bulk splenocytes or purified NK cells were used as effectors and co-cultured with 4T1 tumor cells at a 100:1 effector-to-target ratio. [111]In radioactivity was measured to determine cytotoxic function.

metastases in the lung from IL-15SA/IL-15RαSu-Fc-treated mice decreased significantly ($p < 0.001$) (Figure 7A). Since primary tumors are surgically removed in patients with metastatic breast tumors, we modeled this scenario by performing surgical resection of the 4T1 primary tumor on day 14 and measured survival rates thereafter. Mice treated with IL-15SA/IL-15RαSu-Fc exhibited a significantly higher survival rate ($p = 0.001$), hence greater median overall survival (50 days) than that of the control group (38 days) (Figure 7B), which is in

line with the high anti-metastatic property of IL-15SA/IL-15RαSu-Fc. Next, we wanted to determine which immune population(s) participated in IL-15SA/IL-15RαSu-Fc–induced anti-metastatic activity. CD4$^+$/CD8$^+$ T and NK cell depletions (Figure 7C and 7D) showed that the anti-metastatic property of IL-15SA/IL-15RαSu-Fc appeared to be most dependent on CD8$^+$ T cells but not CD4$^+$ T cells (Figure 7C). Focusing on NK cells, NK depletion abrogated the significant ($p = 0.01$) anti-tumor activity observed between non-treated and IL-15SA/IL-15RαSu-
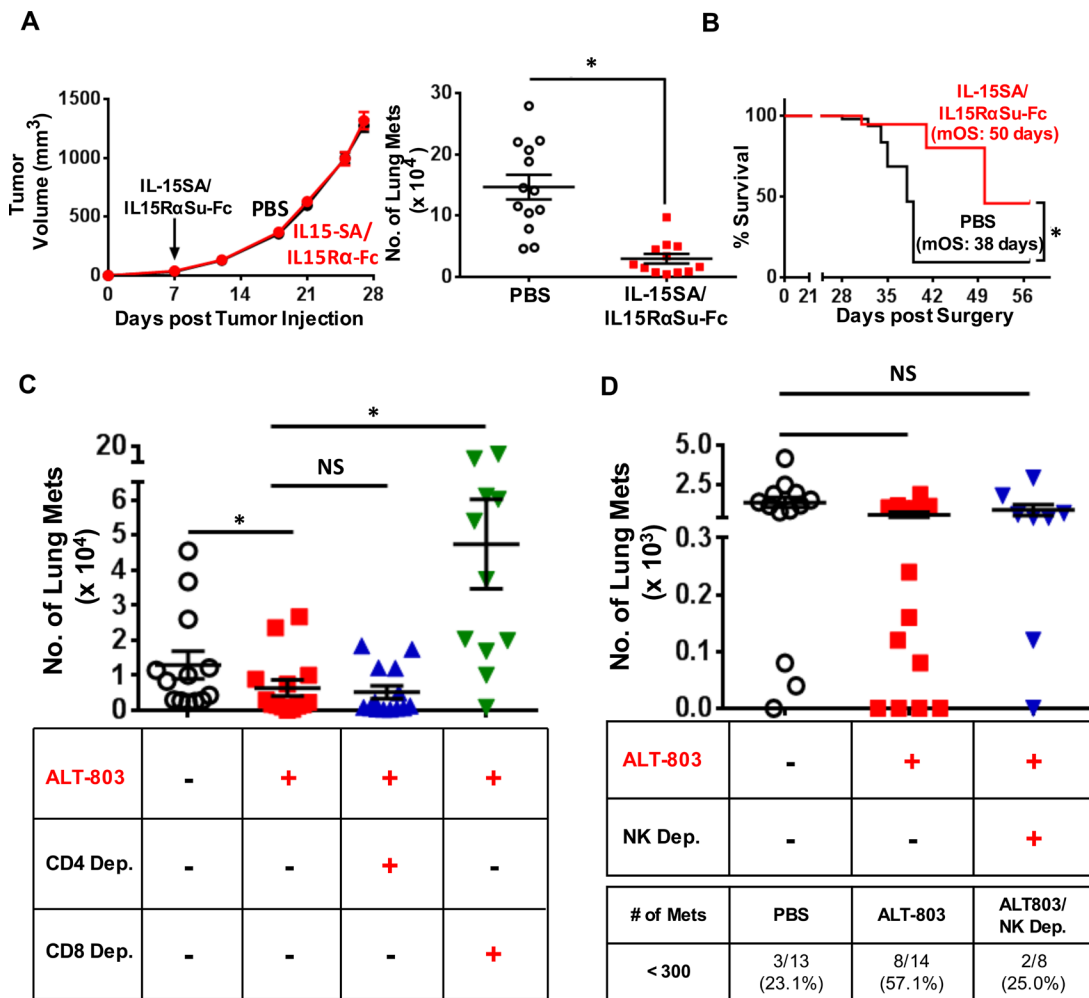

Figure 7: IL-15SA/IL-15RαSu-Fc shows significant anti-metastatic activity, dependent on CD8$^+$ T and NK cells, and prolonged the survival of mice in the 4T1 breast tumor model. A. Female Balb/c mice (n = 15/group) received 4T1 mammary tumor cells, followed by administration of IL-15SA/IL-15RαSu-Fc or PBS on day 7 post–tumor implantation. Primary tumor volume was measured once or twice per week, and the lungs were harvested and analyzed for pulmonary clonogenic cells when the tumor size reached ~1200 mm³. *$p < 0.05$, statistical significance determined by the two-tailed Mann-Whitney U test. **B.** For the survival study, 4T1 tumor implantation and IL-15SA/IL15RαSu-Fc or PBS administration were performed as in (A). Primary tumors were excised on day 14 post 4T1 implantation, then the survival rates of IL-15SA/IL-15RαSu-Fc–treated (n = 6) and PBS-treated (n = 9) mice were examined. Median overall survival (mOS) for each group is shown. *$p < 0.05$, statistical significance determined by the Gehan-Breslow-Wilcoxon test. For **C.** T cell and **D.** NK cell depletions, 4T1 tumor implantation and IL-15SA/IL-15RαSu-Fc (ALT-803) or PBS administration were performed as in (A). Anti-CD8 (Clone 2.43) and anti-CD4 (GK 1.5) mAbs were used to deplete CD8$^+$ and CD4$^+$ T cells, respectively. Anti-asialo-GM1 Ab was used to deplete NK cells. Clonogenic metastatic analysis was performed as in (A). Also shown in (D) is the percentage of mice for each treatment group that had less than 300 metastases. Error bars represent SE of mean of number of clonogenic metastasis per group. *$p < 0.05$, statistical significance determined by the two-tailed Mann-Whitney U test. NS: no significance determined by the two-tailed Mann-Whitney U test.

Fc–treated mice (Figure 7D). The role of NK cells was most evident in the proportion of mice that had less than 300 metastases (Figure 7D, untreated mice vs. NK depleted IL-15SA/IL-15RαSu-Fc–treated mice, $p = 0.09$). These data are consistent with the published *in vivo* data pertaining to IL-15SA/IL15RαSu-Fc, which have shown that its mediation of anti-tumor and viral responses is dependent on CD8^{+} T and/or NK cells [16–18, 26]. Furthermore, these data correlate with the kinetic analysis of IL-15SA/IL-15RαSu-Fc–induced immune responses shown earlier, as NK and CD8^{+} T cell populations were most expanded by IL-15SA/IL-15RαSu-Fc administration (Figure 2).

IL-15SA/IL-15RαSu-Fc therapy, particularly in conjunction with anti-CTLA-4 treatment, resulted in increased survival against experimental pulmonary metastasis of CT26 colon carcinoma cells

We tested the anti-tumor efficacy of IL-15SA/IL-15RαSu-Fc in an additional experimental metastasis tumor model using CT26 colon carcinoma cells. In a side-by-side survival study with rIL-15, we have shown that IL-15SA/IL-15RαSu-Fc generated a significantly higher anti-tumor activity than rIL-15 and prolonged survival against CT26 pulmonary metastasis [15]. In this study, we then examined the combination potential of IL-15SA/IL-15RαSu-Fc with the checkpoint inhibitors anti-CTLA-4 and anti-PD-L1. CT26 cells, similar to 4T1, have a very low level of PD-L1, but unlike 4T1, they highly express the CTLA-4 ligand, B7-1, on the surface [27–29]. To validate these findings, CT26 cells were stained with fluorochrome-labeled antibodies specific for PD-L1 and CTLA-4, followed by a flow cytometry analysis, which confirmed the poor expression of PD-L1 (2.24%) but significant expression of B7-1 (30.5%) on CT26 tumor cells (Figure 8A). In addition, we examined PD-L1 and B7-1 expressions on 4T1 and CT26 *in-vitro* and found that PD-L1, but not B7-1, expression was elevated in these cells after IFNγ treatment (Supplemental Figure 2). The results revealed that IL-15SA/IL-15RαSu-Fc when administered in combination with anti-CTLA-4, but not anti-PD-L1, synergistically increased survival of CT26-bearing mice ($p < 0.01$), (Figure 8B). Finally, we wanted to determine whether anti-PD-L1, albeit ineffective in combination with IL-15SA/IL-15RαSu-Fc (Figure 8B), provided survival benefit when incorporated into the combination treatment of IL-15SA/IL-15RαSu-Fc and anti-CTLA-4. The addition of anti-PD-L1 trended to improve the IL-15SA/IL-15RαSu-Fc plus anti-CTLA-4 treatment in the survival of CT26-bearing mice (Figure 8C). The same triple combination strategy, using rIL-15, was less effective than even IL-15SA/IL-15RαSu-Fc treatment alone (Figure 8C). Overall, administration of IL-15SA/IL-15RαSu-Fc exhibited a potent anti-metastatic activity against not only 4T1 breast (Figure 7) but also CT26 colon carcinoma (Figure 8), and produced a synergistic anti-tumor response against CT26 pulmonary metastasis in combination with checkpoint inhibitors, driven mainly by anti-CTLA-4.

DISCUSSION

To our knowledge, the results shown here report for the first time that IL-15SA/IL-15RαSu-Fc significantly promoted the development of "high effector" NK cells (Figure 4), which increased not only total function but also per-cell function of NK cells (Figure 5). In addition, IL-15SA/IL-15RαSu-Fc induced high levels of inflammatory cytokines, particularly IFN-γ (Figure 1), and promoted the development of innate memory CD8^{+} T cells expressing NKG2D (Figure 3); the latter immune response is a unique property of IL-15SA/IL-15RαSu-Fc that rIL-15 does not possess [14, 16]. We also demonstrate for the first time that IL-15SA/IL-15RαSu-Fc exhibited potent anti-metastatic activity, dependent on CD8^{+} T and NK cells, and prolonged the survival of mice, initially in the 4T1 breast tumor model, which resembles advanced breast cancer in humans (Figure 7). This anti-metastatic property of IL-15SA/IL-15RαSu-Fc was again exhibited in a second tumor metastasis model, involving CT26 colon carcinoma cells, with which we showed for the first time that the metastatic inhibition by IL-15SA/IL-15RαSu-Fc was more potent than that of rIL-15 (Figure 8A) and could be synergized with checkpoint inhibitors (Figure 8B and 8C). The studies reported here further define mechanistically the prior immune and anti-tumor studies of IL-15SA/IL-15RαSu-Fc [16–18].

Acute clinical toxicities have been a major concern for native rIL-15 administration due to highly elevated levels of pro- and anti-inflammatory cytokines such as IFN-γ, IL-6, TNF-α, and IL-10 [8]. In our murine model using a single intraperitoneal (i.p.) injection of 1 μg IL-15SA/IL-15RαSu-Fc, we also observed significant elevations of IFN-γ, TNF-α, and IL-10 (Figure 1A), but not IL-6 (Figure 1A; inset), which interestingly showed the greatest fold increase in the phase I clinical study of rhIL-15 [8] and was determined to be a primary cytokine mediator of toxicity in leukemia patients treated with chimeric antigen receptor effector cells [30, 31]. In our preclinical study, a single i.p. administration of 1 μg IL-15SA/IL-15RαSu-Fc significantly increased levels of inflammatory cytokines, but mice showed no observable toxicities at this dose (as determined by clinical observation and animal weights), possibly due to no significant change in serum IL-6 level (Figure 1A; inset). Our data reported here using Balb/c mice are consistent with data recently reported of an extensive non-clinical toxicity and pharmacodynamic studies of IL-15SA/IL-15RαSu-Fc in C57BL/6 mice and non-human primates [15]. Several phase I clinical studies have now

been initiated with IL-15SA/IL-15RαSu-Fc that will also examine the levels of induced Th1 and Th2 cytokines.

Besides its increased potency and longer half-life compared with native IL-15 [11], IL-15SA/IL-15RαSu-Fc was shown to induce innate memory CD8^{+}

T cells capable of non-antigen–specific killing in murine myeloma models [14, 16]. Our results are consistent with the published findings [14, 16], as we also found that IL-15SA/IL-15RαSu-Fc significantly increased IL-15 memory responders (CD122^{+} CD44^{+}) in the CD8^{+} T
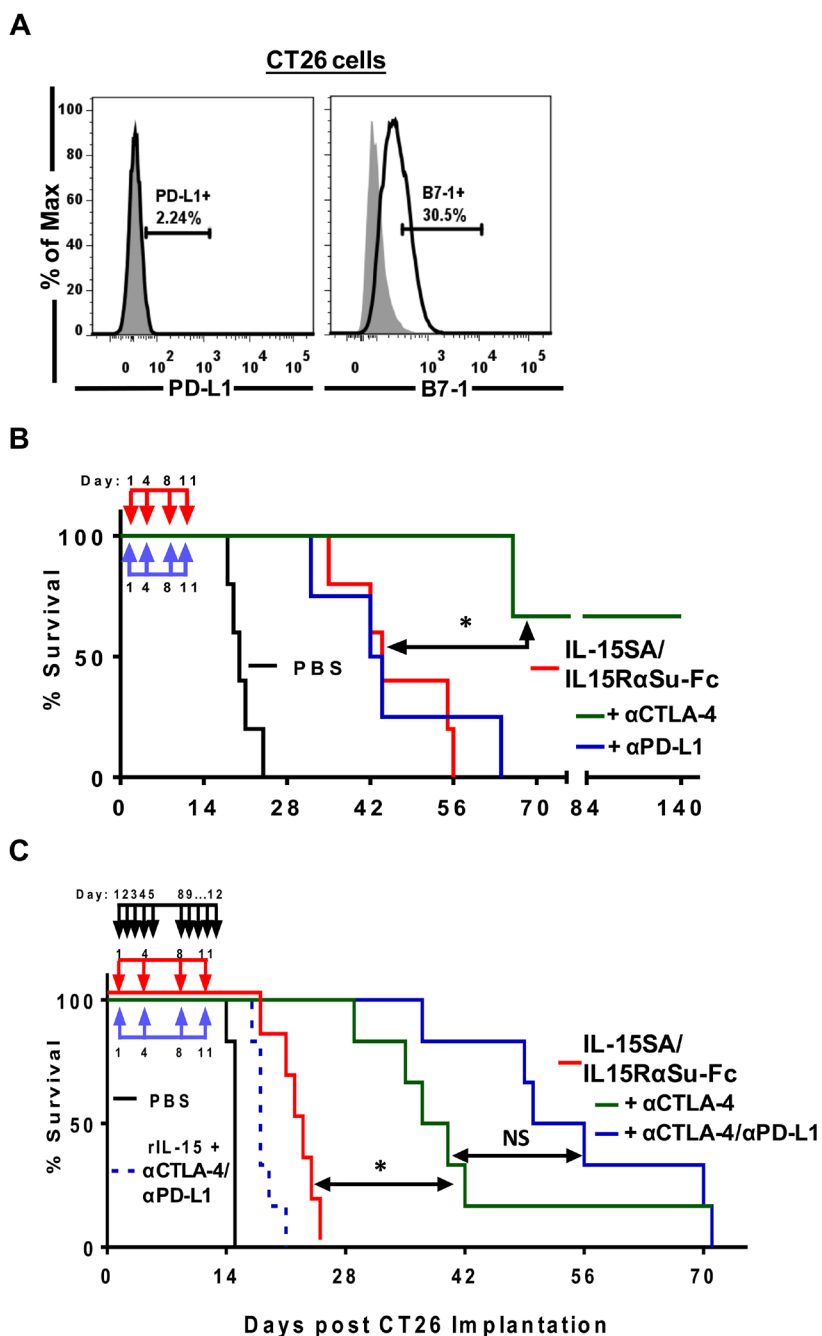

Figure 8: IL-15SA/IL-15RαSu-Fc prolongs the survival of mice against experimental pulmonary metastasis of CT26 colon carcinoma cells and in combination with checkpoint inhibitors, driven by anti-CTLA-4, resulted in synergistic enhancement of anti-tumor efficacy. A. Surface expressions of PD-L1 and B7-1 (black lines) on CT26 cells were analyzed by flow cytometry. Isotype controls are shown in filled grey histograms. **B.** IL-15SA/IL-15RαSu-Fc (red down arrow) treated mice concurrently received either anti-CTLA-4 or anti-PD-L1 (blue up arrow), and their survival rates were measured. **C.** Mice received anti-CTLA-4 or in combination with anti-PD-L1 (blue up arrow) concurrently with IL-15SA/IL-15RαSu-Fc (red down arrow), and their survival was monitored. Also shown are mice that received rIL-15 (black down arrow) plus anti-CTLA-4/anti-PD-L1. *$p < 0.05$, statistical significance; NS: no significance determined by Gehan-Breslow-Wilcoxon test.

cell compartment, in particular those having the innate (NKG2D$^+$) phenotype (Figure 3). Notably, the kinetic profile of innate IL-15 memory responders in the CD8$^+$ T cell population was very similar to that of NK cells (Figures 2 and 3), confirming the notion that IL-15SA/IL-15RαSu-Fc prevalently activates the innate arm of the immune response.

The subsets of CD8$^+$ T cells such as IL-15 memory responders have been extensively described phenotypically and functionally [32–37]. However, significantly less analysis has been carried out on subpopulations of NK cells, which, unlike T cells, are classically considered non-antigen-specific and have no well-defined memory development [38, 39]. Because murine NK cells when exposed to IL-15SA/IL-15RαSu-Fc *in vivo* responded the highest among major immune cells in terms of total number and fold increase (Figure 2), it became a prerequisite to analyze the subsets of NK cells, particularly on day 3 post–cytokine complex treatment. We observed that IL-15SA/IL-15RαSu-Fc significantly promoted the development of "high effector" (CD11b$^+$ CD27^{hi}) NK cells, peaking on day 3 post cytokine complex treatment. It is interesting to note that the level of high effector NK cells returned to the baseline by day 7, whereas the significant level of "terminal effector" (CD11b$^+$ CD27^{lo}) NK cells still remained above the baseline (Figure 4A), indicative of the greater migratory capacity of high effector NK cells for tissue infiltration [21, 22].

Prior to the NK subset analysis mentioned above, we originally hypothesized that IL-15SA/IL-15RαSu-Fc would not have a significant impact on the per-cell function of NK cells, as nearly all NKs in naive Balb/c mice (day 0) showed an activated phenotype (~80% of CD49b$^+$ NKs were CD122$^+$NKp46$^+$) and maintained similar levels of the activated state throughout the *in vivo* kinetics study of immune cells exposed to IL-15-SA/IL-15Rα (Figure 4). As expected, IL-15SA/IL-15RαSu-Fc increased total splenic NK activity (Figure 5A). Unexpectedly, the significant increase in per-cell function of NK cells was observed (Figure 5B). We found that the effect of ALT-803 on NK and CD8+ T cells in tumor-bearing mice (Figure 6) was very similar to those in tumor-free mice (Figure 2). Regulatory T cells and monocytes/monocytic-MDSCs in tumor bearing mice also showed similar results as in tumor-free mice. As seen in tumor-free mice, ALT-803 significantly increased the number of neutrophils/granulocytic MDSCs in tumor bearing mice (Figure 6).

We attribute this enhanced per-cell function to increased development of high effector NK cells induced by IL-15-SA/IL-15RαSu-Fc. This finding also underscores the need for in-depth phenotypic and functional analyses of NK cell subsets. Adding to the potential complexity of these subsets, a cytometry by time of flight (CyTOF) analysis of human NKs revealed that there were 30,000 unique NK cell subsets found in 22 healthy individuals [40]. It has been postulated that this enormous number of unique NK subsets can be categorized on the basis of their ability to protect against different types of pathogens and, perhaps, also tumors [40–42].

We used two highly metastatic tumor models to examine the anti-tumor efficacy of IL-15-SA/IL-15RαSu-Fc. First, in the 4T1 breast tumor model, IL-15SA/IL-15RαSu-Fc was effective in reducing lung metastases, dependent on CD8$^+$ T as well as NK cells, and increased the median overall survival from 38 to 50 days post–surgical resection of the primary tumor (Figure 7). In our study, CD8$^+$ T cells and NK cells played a prominent role in inhibiting pulmonary 4T1 metastasis (Figure 7C and 7D). Because IL-15SA/IL-15RαSu-Fc significantly induces the expansion of high effector NK cells (Figure 4), which have been shown to express a high level of CXCR3 [21, 22] and exhibit superior migratory capacity [21, 22], incorporating IL-15SA/IL-15RαSu-Fc into a vaccine-based immunotherapy may synergistically enhance priming and activation of tumor-antigen specific T cells, mediated by this subpopulation of NK cells.

Next, we employed the CT26 pulmonary metastasis model not only to determine the extent to which the anti-metastatic property of IL-15SA/IL-15RαSu-Fc could be applied to a different tumor type, but also to combine IL-15SA/IL-15RαSu-Fc with an immune checkpoint therapy using, for example, anti-CTLA-4 or anti-PD-L1 antibodies. The immune checkpoint receptor ligands B7-1 and PD-L1 are upregulated on certain tumors and have been shown to inhibit T cell function by contributing to the tumor's ability to evade the immune system [43]. Thus, checkpoint inhibitors such as anti-CTLA-4 and anti-PD-1 or anti-PD-L1 antibodies can enhance T cell responses by breaking peripheral tolerance and preventing immune exhaustion [43, 44]. Additional combination therapies with immunostimulatory agents such as IL-15SA/IL-15RαSu-Fc, which promotes T cell proliferation and enhances their cytotoxicity, can potentially provide synergistic anti-tumor responses. In contrast to 4T1 tumor cells, which did not markedly express B7-1 and PD-L1, CT26 tumor cells expressed a low level of PD-L1 but a high level of B7-1 (see Results); hence their practicability for immune checkpoint combination therapy, specifically with anti-CTLA-4. Administration of IL-15SA/IL-15RαSu-Fc and anti-CTLA-4, but not anti-PD-L1, generated a synergistic anti-tumor response in CT26-bearing mice (Figure 8B), which is consistent with the observation that the efficacy of checkpoint inhibitors, in particular anti-PD-1 and PD-L1, is dependent on the surface expression of inhibitory ligands on tumor cells [45–47]. More interestingly, anti-PD-L1, albeit ineffective in combination with IL-15SA/IL-15RαSu-Fc in this tumor model, appeared to further improve survival when administered in conjunction with both IL-15SA/IL-15RαSu-Fc and anti-CTLA-4 (Figure 8C). We believe that CTLA-4/B7-1 blockade via anti-CTLA-4 induced IFN-γ secretion not only from T cells, but also from NK cells, which have been shown to express CTLA-4 in mediating IFN-γ production [48]. This likely resulted in increased

expression of PD-L1 on CT26 tumor cells, rendering anti-PD-L1 efficacious. Our studies combining the IL-15 reagent with anti-CTLA-4 and/or PDL1 reflect our vision that the most effective therapies will be in combination with the emerging checkpoint inhibitors. We feel that increased survival in the CT26 tumor model (and control of macroscopic disease in the 4T1 model) can be further optimized by timing and sequencing of these reagents.

In conclusion, the results shown here support the use of IL-15SA/IL-15RαSu-Fc for anti-metastatic treatment against common non-hematologic tumors such as breast and colon carcinomas. Because IL-15SA/IL-15RαSu-Fc predominantly activated the innate arm of the immune system (Figures 2–4), a combination strategy involving the reagents that stimulate the adaptive arm of anti-tumor immunity, in particular recombinant vaccines or checkpoint inhibitors demonstrated in this study, may prove to be highly effective in the treatment of metastatic cancers.

MATERIALS AND METHODS

Animals

Female Balb/c mice were housed and maintained in microisolator cages under specific pathogen-free conditions and in accordance with the Association for Assessment and Accreditation of Laboratory Animal Care guidelines. All experimental studies were carried out under the approval of the National Institutes of Health (NIH) Intramural Animal Care and Use Committee.

Tumor cells

4T1 murine mammary and CT26 murine colon carcinoma cell lines were purchased from American Type Culture Collection and maintained in the recommended medium.

IL-15SA/IL-15RαSu-Fc (ALT-803) reagent

IL-15SA/IL-15RαSu-Fc (ALT-803) was generated as described previously [11] and kindly provided by Altor BioScience Corporation (Miramar, FL) under a Cooperative Research and Development Agreement (CRADA).

Kinetic analysis of IL-15-SA/IL-15Rα-Fc–mediated immune responses

For each day, a group of naïve female Balb/c mice (n=3) was injected only once with IL-15SA/IL15-RαSu-Fc (1 μg in 100 μl, i.p.); their sera and spleens, including those from the control-PBS group (n = 3), were collected on day 7. Mouse sera were characterized for TH_1 and TH_2 cytokines using a cytokine multiplex analysis (Clinical Support Laboratory, NCI-Frederick). Mouse spleens were passed through a 70μM cell strainer and homogenized into a single cell suspension, followed by alkaline lysis of red blood cells, for antibody staining and flow analysis.

Flow cytometry analysis; surface and intracellular marker assays

An LSR Fortessa (BD Biosciences, Franklin Lakes, NJ) was used for multiparametric flow cytometry analysis. A Live/Dead Fixable Blue Dead Cell Stain Kit (Molecular Probes; Thermo Fisher Scientific, Grand Island, NY) was used to exclude dead cells. The following murine monoclonal antibodies (mAbs) were used to stain Balb/c splenocytes to characterize immune cell subsets: FITC-CD8 (Clone 53-6.7; BD Biosciences), PE-CD49b (Clone DX5; BioLegend, San Diego, CA), PE-PD-L1 (Clone 10F.9G2; BioLegend), PerCP-Cy5.5-B7-1 (Clone 16-10A1; BioLegend), PerCP-Cy5.5-FOXP3 (Clone FJK-16s; eBioscience, San Diego, CA), PE-Cy7-CD122 (Clone Tm-b1; eBioscience), APC-NKG2D (Clone CX5; BioLegend), APC-Cy7-CD3 (Clone 17A2; BioLegend), Pacific Blue-CD44 (Clone IM7; BioLegend), AF700-CD4 (Clone GK1.5; eBioscience), BV605-CD19 (Clone 6D5; BioLegend), BV605-PD-1 (Clone 29F.1A12; BioLegend), BV510-NKp46 (Clone 29A1.4; BioLegend), Pacific Blue-CD27 (Clone LG.3A10; BioLegend), FITC-CD11b (Clone M1/70; BD Biosciences), AF700-CD11b (Clone M1/70; BioLegend), APC-Cy7-CD11c (Clone N418; BioLegend), BV510-CD3 (Clone 17A2; BioLegend), Pacific Blue-Ly6-G (Clone 1A8; BioLegend), BV605-Ly6-C (Clone HK1.4; BioLegend).

NK cytotoxicity assay

Female Balb/c mice (n = 5–10/group) were given a single injection of IL-15SA/IL-15RαSu-Fc (1 μg in 100 μl, i.p.) or PBS (100 μl i.p.). On day 3, their spleens were harvested and processed as above. Mouse splenocytes were either used as effectors or purified for NK cells using the NK Cell Isolation Kit II (Miltenyi Biotec, San Diego, CA). YAC-1 target cells were labeled with ^{111}In and co-cultured with bulk splenocytes or purified NK cells at 100:1, 10:1, and 1:1 effector-to-target ratios. For the NKG2D blocking assay, anti-mouse NKG2D (10 μg/ml; R&D Systems, Minneapolis, MN) or isotype control mAb was added to NK cells, incubated at room temperature for 20 min, then ^{111}In-labeled YAC-1 cells were added. After incubation at 37° C for 4 hours, radioactivity in supernatant was measured using a γ counter (WIZARD[2]; PerkinElmer, Waltham, MA). Where indicated, NK activity was converted to lytic units (LU), as described by Wunderlich et al. [49].

T/NK cell depletion study

Female Balb/c mice (n=15/group) were injected with 4T1 mammary tumor cells and given IL-15SA/IL-15RαSu-Fc (1 μg in 100 μl, i.p.) or PBS (100 μl i.p.) as above. T cell depletion was started on the day of tumor implantation using a daily dose (100 μg, i.p.) of anti-CD4 (Clone GK1.5) or anti-CD8 (Clone 2.43), purchased from BioXcell (West Lebanon, NH) for first the 3 days and once

a week thereafter until harvest of the lungs (days 25–29). For NK depletion using anti-Asialo-GM1, it was reported that the greatest reduction of NK cell activity was seen on day 3 after one-shot injection, recovered on day 7, and rose to more than 50% of the original value on day 14 in nude and Balb/c mice [50]. Therefore, the following depletion schedule was used: briefly, 10 µl of anti-Asialo-GM1 (Wako Chemicals USA, Inc., Richmond, VA), diluted 1:5 in PBS, was injected 100 µl i.p. 1 day prior to IL-15SA/IL-15RαSu-Fc administration, then thereafter every 5-6 days until harvest of the lungs (days 25–30). The percent depletions of T and NK cells was checked on the day prior to IL-15SA/IL-15RαSu-Fc administration (CD4: 98.6%; CD8: 97.4%; NK: 91.6%) and 4 days after the last injection (CD4: 87.1%; CD8: 77.1%; NK: 33.7%).

4T1 anti-tumor and survival study

Female Balb/c mice (n = 15/group) were injected with 5 x 10^4 4T1 mammary tumor cells. Seven days after implantation, IL-15SA/IL-15RαSu-Fc (1 µg in 100 µl, i.p.) or PBS (100 µl i.p.) was administered. Tumors were measured twice a week. When the tumor volume (L x W^2/2) reached 1000-1200 mm^3, mice were euthanized, and their lungs were harvested and dispersed into single cell suspension, which was plated in the presence of 6-thioguanine (Sigma-Aldrich, St. Louis, MO). Twelve days later, cells were fixed with methanol, stained with 0.03% methylene blue, and the number of clonogenic metastatic cells was counted. For the survival study, primary tumors were surgically removed on day 14 post 4T1 implantation, then the survival of IL-15-SA/IL-15Rα-Fc-treated (N=6) or PBS-treated (N=9) mice was examined. Mice where surgery failed to control primary tumor (Dia. > 1.9 cm) after tumor resection were excluded for the survival analysis.

CT26 anti-tumor and survival study

Female Balb/c mice (n = 6–8/group) were injected with 2x 10^5 CT26 tumor cells intravenously (i.v.) on day 0. Treatment began 1 day later. In the rIL-15 treatment group, each mouse received 5 µg of rIL-15 (NCI, lot #: L0810009, Conc: 0.59 mg/ml, DOM: 12/03/08) i.p. daily, five times a week for 2 weeks. Along with rIL-15, animals also received both anti-mouse-PD-L1 antibody (clone 9G2; Biolegend) and anti-CTLA-4 antibody (clone UC10-4F10-11; Altor). In the IL-15SA/IL-15RαSu-Fc treatment group, each mouse received 4 µg of IL-15SA/IL-15RαSu-Fc i.v. twice a week. Along with IL-15-SA/IL-15RαSu-Fc, some mice receive either anti-mouse-PD-L1 antibody, anti-CTLA-4 antibody or both anti-mouse-PD-L1 and anti-CTLA-4 antibodies. The dose and schedule of these antibodies were 100 µg per injection administered twice a week for 2 weeks. Control mice received injections of PBS. Survival was set as an endpoint, and mice were monitored for weight changes thrice a week until the termination of the study.

Statistical analysis

Unless specified, results of tests of significance are indicated as p values derived from a two-tailed Student's t test. All p values were derived at 95% using GraphPad Prism 6 statistical software for PCs (GraphPad Software, Inc., La Jolla, CA).

CONFLICTS OF INTEREST

P. Kim A. Kwilas, J. Schlom and J. Hodge are employees of the Laboratory of Tumor Immunology and Biology, NCI, NIH, DHHS and have no conflicts to disclose. W. Xu, S. Alter, E. Jeng, and H. Wong are employees and stockholders of Altor BioScience Corporation.

Abbreviations

AICD, activation-induced cell death; conv., conventional; CyTOF, cytometry by time of flight; IL, interleuken; IL-15SA/IL-15RαSu-Fc; ALT-803, IL-15 superagonist/IL-15RαSushi-Fc fusion complex; IFN-γ, interferon gamma; ^{111}In, indium 111; i.p., intraperitoneal; i.v., intravenously; LU, lytic units; MAb, monoclonal antibody; MDSC, myeloid derived suppressor cell; MHC, major histocompatibility complex; mOS, median overall survival; NCI, National Cancer Institute; NIH, National Institutes of Health; NK, natural killer; NS, no significance; PBS, phosphate buffered saline; rh, recombinant human; TCR, T cell receptor; TNFα, tumor necrosis factor alpha, Tregs; regulatory T cells.

REFERENCES

1. Tagaya Y, Bamford RN, DeFilippis AP, Waldmann TA. IL-15: a pleiotropic cytokine with diverse receptor/signaling

pathways whose expression is controlled at multiple levels. Immunity. 1996; 4:329-336.

2. Ma A, Boone DL, Lodolce JP. The pleiotropic functions of interleukin 15: not so interleukin 2-like after all. J Exp Med. 2000; 191:753-756.

3. Maloy KJ, Powrie F. Fueling regulation: IL-2 keeps CD4+ Treg cells fit. Nat Immunol. 2005; 6:1071-1072.

4. Fontenot JD, Rasmussen JP, Gavin MA, Rudensky AY. A function for interleukin 2 in Foxp3-expressing regulatory T cells. Nat Immunol. 2005; 6:1142-1151.

5. D'Cruz LM, Klein L. Development and function of agonist-induced CD25+ Foxp3+ regulatory T cells in the absence of interleukin 2 signaling. Nat Immunol. 2005; 6:1152-1159.

6. Marks-Konczalik J, Dubois S, Losi JM, Sabzevari H, Yamada N, Feigenbaum L, Waldmann TA, Tagaya Y. IL-2-induced activationinduced cell death is inhibited in IL-15 transgenic mice. Proc Natl Acad Sci U S A. 2000; 97:11445-11450.

7. Waldmann TA. The biology of interleukin-2 and interleukin-15: implications for cancer therapy and vaccine design. Nature reviews Immunology. 2006; 6:595-601.

8. Conlon KC, Lugli E, Welles HC, Rosenberg SA, Fojo AT, Morris JC, Fleisher TA, Dubois SP, Perera LP, Stewart DM, Goldman CK, Bryant BR, Decker JM, Chen J, Worthy TA, Figg WDS, et al. Redistribution, hyperproliferation, activation of natural killer cells and CD8 T cells, and cytokine production during first-in-human clinical trial of recombinant human interleukin-15 in patients with cancer. J Clin Oncol. 2015; 33:74-82.

9. Kobayashi H, Carrasquillo JA, Paik CH, Waldmann TA, Tagaya Y. Differences of biodistribution, pharmacokinetics, and tumor targeting between interleukins 2 and 15. Cancer Research. 2000; 60:3577-3583.

10. Zamai L, Ponti C, Mirandola P, Gobbi G, Papa S, Galeotti L, Cocco L, Vitale M. NK cells and cancer. J Immunol. 2007; 178:4011-4016.

11. Han KP, Zhu X, Liu B, Jeng E, Kong L, Yovandich JL, Vyas VV, Marcus WD, Chavaillaz PA, Romero CA, Rhode PR, Wong HC. IL-15:IL-15 receptor alpha superagonist complex: high-level co-expression in recombinant mammalian cells, purification and characterization. Cytokine. 2011; 56:804-810.

12. Rubinstein MP, Kovar M, Purton JF, Cho JH, Boyman O, Surh CD, Sprent J. Converting IL-15 to a superagonist by binding to soluble IL-15R{alpha}. Proc Natl Acad Sci U S A. 2006; 103:9166-9171.

13. Stoklasek TA, Schluns KS, Lefrancois L. Combined IL-15/IL-15Ralpha immunotherapy maximizes IL-15 activity in vivo. J Immunol. 2006; 177:6072-6080.

14. Wong HC, Jeng EK, Rhode PR. The IL-15-based superagonist ALT-803 promotes the antigen-independent conversion of memory CD8+ T cells into innate-like effector cells with antitumor activity. Oncoimmunology. 2013; 2:e26442.

15. Rhode PR, Egan JO, Xu W, Hong H, Webb GM, Chen X, Liu B, Zhu X, Wen J, You L, Kong L, Edwards AC, Han K, Shi S, Alter S, Sacha JB, et al. Comparison of the Superagonist Complex, ALT-803, to IL15 as Cancer Immunotherapeutics in Animal Models. Cancer Immunol Res. 2016; 4:49-60.

16. Xu W, Jones M, Liu B, Zhu X, Johnson CB, Edwards AC, Kong L, Jeng EK, Han K, Marcus WD, Rubinstein MP, Rhode PR, Wong HC. Efficacy and mechanism-of-action of a novel superagonist interleukin-15: interleukin-15 receptor alphaSu/Fc fusion complex in syngeneic murine models of multiple myeloma. Cancer Res. 2013; 73:3075-3086.

17. Gomes-Giacoia E, Miyake M, Goodison S, Sriharan A, Zhang G, You L, Egan JO, Rhode PR, Parker AS, Chai KX, Wong HC, Rosser CJ. Intravesical ALT-803 and BCG treatment reduces tumor burden in a carcinogen induced bladder cancer rat model; a role for cytokine production and NK cell expansion. PLoS one. 2014; 9:e96705.

18. Mathios D, Park CK, Marcus WD, Alter S, Rhode PR, Jeng EK, Wong HC, Pardoll DM, Lim M. Therapeutic administration of IL-15 superagonist complex ALT-803 leads to long-term survival and durable antitumor immune response in a murine glioblastoma model. Int J Cancer. 2016; 138:187-194.

19. Leclercq G, Debacker V, de Smedt M, Plum J. Differential effects of interleukin-15 and interleukin-2 on differentiation of bipotential T/natural killer progenitor cells. J Exp Med. 1996; 184:325-336.

20. Hayakawa Y AD, Smyth MJ. Subset analysis of human and mouse mature NK cells. Methods Mol Biol 2010; 612:27-38.

21. Hayakawa Y, Huntington ND, Nutt SL, Smyth MJ. Functional subsets of mouse natural killer cells. Immunological reviews. 2006; 214:47-55.

22. Hayakawa Y, Smyth MJ. CD27 dissects mature NK cells into two subsets with distinct responsiveness and migratory capacity. J Immunol. 2006; 176:1517-1524.

23. Huntington ND, Tabarias H, Fairfax K, Brady J, Hayakawa Y, Degli-Esposti MA, Smyth MJ, Tarlinton DM, Nutt SL. NK cell maturation and peripheral homeostasis is associated with KLRG1 up-regulation. J Immunol. 2007; 178:4764-4770.

24. Ardiani A, Gameiro SR, Palena C, Hamilton DH, Kwilas A, King TH, Schlom J, Hodge JW. Vaccine-mediated immunotherapy directed against a transcription factor driving the metastatic process. Cancer Res. 2014; 74:1945-1957.

25. Pulaski BA, Ostrand-Rosenberg S. Mouse 4T1 breast tumor model. Current protocols in immunology / edited by John E Coligan [et al]. 2001; Chapter 20:Unit 20 22.

26. Seay K, Church C, Zheng JH, Deneroff K, Ochsenbauer C, Kappes JC, Liu B, Jeng EK, Wong HC, Goldstein H. In Vivo Activation of Human NK Cells by Treatment with an Interleukin-15 Superagonist Potently Inhibits Acute In Vivo HIV-1 Infection in Humanized Mice. Journal of virology. 2015; 89:6264-6274.

27. Ruocco MG, Pilones KA, Kawashima N, Cammer M, Huang J, Babb JS, Liu M, Formenti SC, Dustin ML, Demaria S. Suppressing T cell motility induced by anti-CTLA-4 monotherapy improves antitumor effects. The Journal of clinical investigation. 2012; 122:3718-3730.

28. Sagiv-Barfi I, Kohrt HE, Czerwinski DK, Ng PP, Chang BY, Levy R. Therapeutic antitumor immunity by checkpoint blockade is enhanced by ibrutinib, an inhibitor of both BTK and ITK. Proc Natl Acad Sci U S A. 2015; 112:E966-972.

29. Tirapu I, Huarte E, Guiducci C, Arina A, Zaratiegui M, Murillo O, Gonzalez A, Berasain C, Berraondo P, Fortes P, Prieto J, Colombo MP, Chen L, Melero I. Low surface expression of B7-1 (CD80) is an immunoescape mechanism of colon carcinoma. Cancer Res. 2006; 66:2442-2450.

30. Brentjens RJ, Davila ML, Riviere I, Park J, Wang X, Cowell LG, Bartido S, Stefanski J, Taylor C, Olszewska M, Borquez-Ojeda O, Qu J, Wasielewska T, He Q, Bernal Y, Rijo IV, et al. CD19-targeted T cells rapidly induce molecular remissions in adults with chemotherapy-refractory acute lymphoblastic leukemia. Science translational medicine. 2013; 5:177ra138.

31. Grupp SA, Kalos M, Barrett D, Aplenc R, Porter DL, Rheingold SR, Teachey DT, Chew A, Hauck B, Wright JF, Milone MC, Levine BL, June CH. Chimeric antigen receptor-modified T cells for acute lymphoid leukemia. The New England journal of medicine. 2013; 368:1509-1518.

32. Banerjee A, Gordon SM, Intlekofer AM, Paley MA, Mooney EC, Lindsten T, Wherry EJ, Reiner SL. Cutting edge: The transcription factor eomesodermin enables CD8+ T cells to compete for the memory cell niche. J Immunol. 2010; 185:4988-4992.

33. Castro I, Yu A, Dee MJ, Malek TR. The basis of distinctive IL-2- and IL-15-dependent signaling: weak CD122-dependent signaling favors CD8+ T central-memory cell survival but not T effector-memory cell development. J Immunol. 2011; 187:5170-5182.

34. Dubois S, Waldmann TA, Muller JR. ITK and IL-15 support two distinct subsets of CD8+ T cells. Proc Natl Acad Sci U S A. 2006; 103:12075-12080.

35. Intlekofer AM, Takemoto N, Wherry EJ, Longworth SA, Northrup JT, Palanivel VR, Mullen AC, Gasink CR, Kaech SM, Miller JD, Gapin L, Ryan K, Russ AP, Lindsten T, Orange JS, Goldrath AW, et al. Effector and memory CD8+ T cell fate coupled by T-bet and eomesodermin. Nat Immunol. 2005; 6:1236-1244.

36. Motegi A, Kinoshita M, Inatsu A, Habu Y, Saitoh D, Seki S. IL-15-induced CD8+CD122+ T cells increase antibacterial and anti-tumor immune responses: implications for immune function in aged mice. Journal of leukocyte biology. 2008; 84:1047-1056.

37. Zuo J, Stohlman SA, Bergmann CC. IL-15-independent antiviral function of primary and memory CD8+ T cells. Virology. 2005; 331:338-348.

38. Lanier LL. NK cell recognition. Annu rev Immunol. 2005; 23:225-274.

39. Vivier E, Tomasello E, Baratin M, Walzer T, Ugolini S. Functions of natural killer cells. Nat Immunol. 2008; 9:503-510.

40. Horowitz A, Strauss-Albee DM, Leipold M, Kubo J, Nemat-Gorgani N, Dogan OC, Dekker CL, Mackey S, Maecker H, Swan GE, Davis MM, Norman PJ, Guethlein LA, Desai M, Parham P, Blish CA. Genetic and environmental determinants of human NK cell diversity revealed by mass cytometry. Science translational medicine. 2013; 5:208ra145.

41. Keener AB. Natural killers: cataloging immune cells for immunotherapy. Nat Med. 2015; 21:207-208.

42. Leavy O. Natural killer cells: a virtual pick and mix. Nat Rev Immunol. 2013; 13:844-845.

43. Perez-Gracia JL, Labiano S, Rodriguez-Ruiz ME, Sanmamed MF, Melero I. Orchestrating immune check-point blockade for cancer immunotherapy in combinations. Current opinion in immunology. 2014; 27:89-97.

44. Kim PS, Ahmed R. Features of responding T cells in cancer and chronic infection. Current opinion in immunology. 2010; 22:223-230.

45. Herbst RS, Soria JC, Kowanetz M, Fine GD, Hamid O, Gordon MS, Sosman JA, McDermott DF, Powderly JD, Gettinger SN, Kohrt HE, Horn L, Lawrence DP, Rost S, Leabman M, Xiao Y, et al. Predictive correlates of response to the anti-PD-L1 antibody MPDL3280A in cancer patients. Nature. 2014; 515:563-567.

46. Mahoney KM, Atkins MB. Prognostic and predictive markers for the new immunotherapies. Oncology (Williston Park). 2014; 3:39-48.

47. Topalian SL, Hodi FS, Brahmer JR, Gettinger SN, Smith DC, McDermott DF, Powderly JD, Carvajal RD, Sosman JA, Atkins MB, Leming PD, Spigel DR, Antonia SJ, Horn L, Drake CG, Pardoll DM, et al. Safety, activity, and immune correlates of anti-PD-1 antibody in cancer. The New England journal of medicine. 2012; 366:2443-2454.

48. Stojanovic A, Fiegler N, Brunner-Weinzierl M, Cerwenka A. CTLA-4 is expressed by activated mouse NK cells and inhibits NK Cell IFN-gamma production in response to mature dendritic cells. J Immunol. 2014; 192:4184-4191.

49. Wunderlich J, Shearer G. (1994). Induction and measurement of cytotoxic T lymphocyte activity. In: Coligan J, Kruisbeek A, Margulies D, Shevach E, Strober W, eds. Current Protocols in Immunology. (Hoboken, NJ: John Wiley and Sons), pp. 3.11.11.

50. Habu S, Fukui H, Shimamura K, Kasai M, Nagai Y, Okumura K, Tamaoki N. In vivo effects of anti-asialo GM1. I. Reduction of NK activity and enhancement of transplanted tumor growth in nude mice. J Immunol. 1981; 127:34-38.